DOI: 10.13009/EUCASS2019-144

Experimental investigation of a single element LOX/GCH4 heat-sink combustion chamber

Christoph B. von Sethe [1], Sebastian Soller [2], Oskar J. Haidn[1]
[1] Institute of Turbomachinery and Flight Propulsion (LTF) – Professorship for Space Propulsion
Technische Universität München (TUM), Boltzmannstraße 15, 85748 Garching b. München, Germany
[2] Ariane Group GmbH, Robert-Koch-Str.1, 82084 Taufkirchen, Germany
christoph.sethe@ltf.mw.tum.de

Abstract

This paper presents results obtained on a rectangular single-injector element combustor, which marks the first step of testing rocket combustion chambers under cryogenic conditions at LTF on subscale level. For this purpose the existing capacitively cooled combustor [1] has been refurbished and equipped with a newly designed injector with a shear coaxial injector without recess and tapering. The tests are executed at 20 and 25 bar chamber pressure in a targeted mixture ratio range from 2.2 to 3.7. Comparison of the tested pressure levels revealed a similar distribution over time and length for the normalized pressure and for the wall temperatures with increased maximum temperatures of 16% for the 25 bar case.
The results will be used to prepare experiments with a multi-injector element chamber featuring the same injector geometry used in the single element combustor.

Nomenclature

A_{hw}	:	Area hot gas wall
C_d-value	:	Discharge coefficient
GCH4	:	Gaseous methane
GN2	:	Gaseous nitrogen
GOX	:	Gaseous oxygen
LN2	:	Liquid nitrogen
LOX	:	Liquid oxygen
$\dot{m}$	:	Mass flow rate (LOX, GCH4 or GN2 (film))
MVHVLOX	:	Digital signal of the magnetic actuator valve of the LOX main valve
nF	:	No film fluid
NTO	:	Nitrous tetroxide
δp_{inj}	:	Average injector pressure drop quotient
Δp_{inj}	:	Injector pressure drop
p_c	:	Chamber pressure
PCabc	:	Static chamber pressure sensor name (abc = number (101 till 109))
PHF	:	High frequency pressure
ROF	:	Propellant mixture ratio
$\dot{q}$	:	Heat flux rate
S	:	Shape factor
ΔT	:	Temperature difference in the chamber wall
TC(L/S)(U/O)yz	:	Chamber wall temperature (L = first segment, S = second segment; U = bottom, O = top; yz = position and wall distance (starting with 01))
TLOX(HV/Inj)	:	LOX bulk temperature at the main valve (HV) or the injector (Inj)
TTurb	:	LOX bulk temperature upstream the measurement turbine
$t_{ref/evaluation}$	:	Reference/Evaluation time for the chamber wall temperatures
u_i	:	Propellant injection velocity
$\dot{V}_{LOX}$	:	LOX volumetric flow rate
VR(F)	:	Velocity ratio propellants (or film)
x	:	Axial distance from the chamber faceplate
$\varepsilon_{c,e}$	:	Nozzle contraction ratio, nozzle expansion ratio
λ	:	Thermal conductivity coefficient
$\theta_{no\ film}$	:	Quotient for the chamber wall temperatures comparing the film influence

DOI: 10.13009/EUCASS2019-144

1. Introduction

For the last years, the propellant combination LOX (liquid oxygen)/methane is under investigation for future rocket applications like space launch or deep space missions. The combination belongs to the group of "Green propellants", for which usage, handling and storage is more ecofriendly, and less expensive than for the storable and toxic combination hydrazine/NTO. For a safe and reliable utilization several technical and scientific studies are necessary [2].
At the research campus of the Technical University of Munich (TUM) in Garching, Germany, the chair of Turbomachinery and Flight Propulsion (LTF) tests rocket thrust chambers on demonstrator and subscale level using gaseous oxygen (GOX) and gaseous methane (GCH4) as propellant. An on-site test facility is suitable to test these chambers up to a chamber pressure of 100 bar with up to 60 s test duration. The combustors feature shear coaxial injectors and are cooled convectively by water [3].
With the goal of expanding experimental and numerical knowledge, the "Bayerische Forschungsstiftung" (BFS) and the industrial partner Ariane Group GmbH have initiated a research project to provide detailed data on LOX/CH4 combustion. Within this project the test facility in Garching has been modified and extended to supply the redesigned single- and multi-injector element combustors with LOX for analysis of heat transfer, combustion efficiency and injector characteristics. Methane is provided in gaseous state.

2. Test specimen

With the current combustor depicted in Fig. 1 chamber pressures of 30 bar can be realized. In this section, a brief description of the combustion chamber and the measurement equipment is presented.

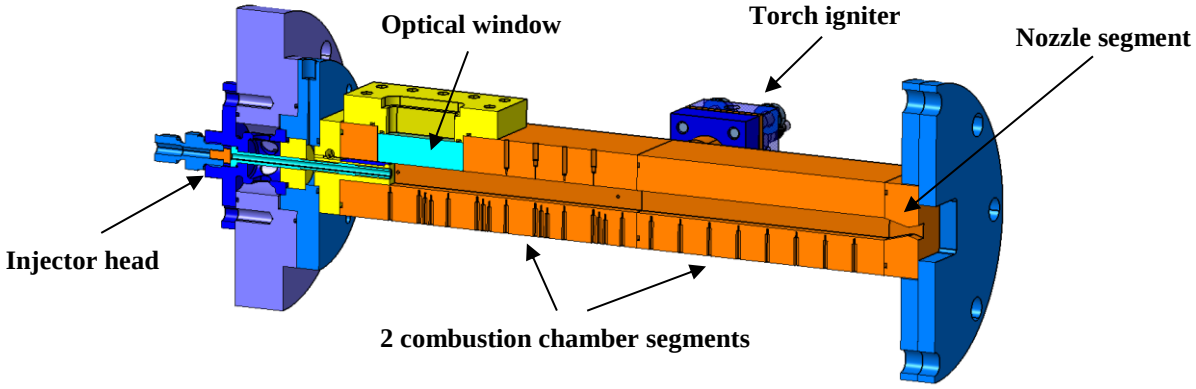

Fig. 1: Combustion chamber with cryogenic injector head and optical access window

2.1 Harware description

Consisting of two chamber segments made of copper[1], the combustion channel is 290 mm long and has a square cross section of 12x12 mm. The convergent-divergent nozzle features a trapezoidal geometry. The contraction ratio is $\varepsilon_c = 2.5$ and the expansion ratio is $\varepsilon_e = 1.62$. Making use of the high thermal conductivity of copper the chamber is cooled capacitively. Thus, operating times of maximum 3 s at 25 bar chamber pressure can be realized.
The chamber is ignited by a separate spark plug torch igniter which is positioned at the end of the first chamber segment (see Fig. 1 and Fig. 4). For optical combustion analysis (see [4, 5]) the chamber can be equipped with an optical window. For the current experiments this is replaced by a copper block, equipped with sheathed thermocouples type K (Electronic Sensor). The sheath is connected to the measurement tip. The propellants are injected via a shear coaxial injector without recess. The methane mass flow is set via a critically flowed orifice. For film cooling of the window, gaseous nitrogen (GN2) is injected via a film applicator (see Fig. 2). The film mass flow is set to 20% of the methane mass flow and is adjusted by an critically flowed orifice.
To homogenize the velocity profile of the inflowing propellants and to provide a certain pressure drop to decouple the injector from the feed system, a porous plate is used for the methane and a metal mesh in the LOX manifold. In purpose of an easy access and exchange the LOX post is only inserted from the left side and fixed by the supply connector (see Fig. 2).

[1] Copper: Cu-HCP (Deoxygenated, high thermal conductivity phosphorous copper (P=20-70ppm))

DOI: 10.13009/EUCASS2019-144

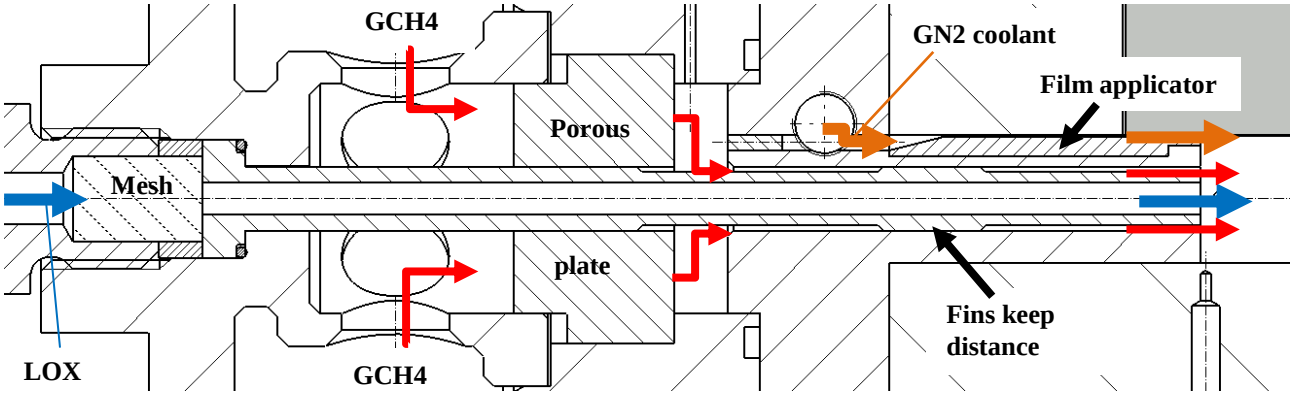

Fig. 2: Coaxial injector element detail view - Flow from left to right

Table 1: Injector dimensions

LOX diameter D_i	3.0	[mm]
LOX post wall thickness w	1.0	[mm]
GCH4 outer diameter	6.0	[mm]
Injector area ratio A_{CH4}/A_{LOX}	1.2	[−]

2.2 Experimental setup

In order to characterize the combustion process, the heat release and the heat transfer to the wall, the chamber is equipped with equally spaced static pressure transducers and spring loaded thermocouples along the chamber axis.
Sheathed thermocouples type T (Electronic Sensor, insultated measurement tip) at 17 positions with a spacing of 17 mm along the chamber axis record the chamber wall bottom temperature at 1 mm distance to the hot gas wall beginning 0.5 mm downstream the faceplate. In addition, thermocouples in 2 mm and 3 mm distance are installed in clusters for heat transfer analysis. For film cooling analysis temperature sensors are placed in the top wall downstream the window assembly in 1 mm distance (see Fig. 3, sample rate = 90 Hz).

The static pressure ("WIKA" sensors, type: A-10, range: 0-40 bar) is measured at nine positions with a spacing of 34 mm along the chamber axis beginning 0.5 mm downstream the faceplate (see Fig. 4, sample rate = 1.5 kHz).
One high frequency pressure sensor (PHF, "Kistler" sensor, type: 6053BB60, range: -100 to +100 bar) mounted to the chamber is able to record the pressure conditions at ignition with a sample rate of 20 kHz.

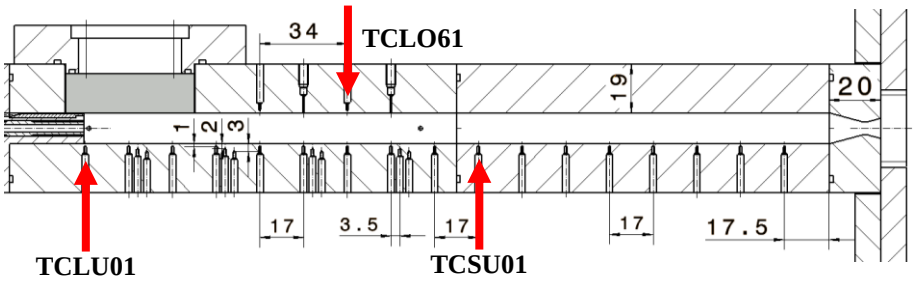

Fig. 3: Chamber wall temperature measurement positions

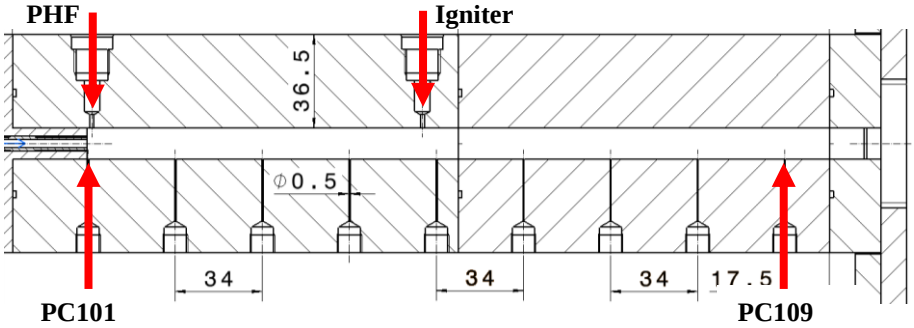

Fig. 4: Static chamber pressure measurement positions

DOI: 10.13009/EUCASS2019-144

Fig. 5 presents the simplified fluid supply of the LOX line. The volumetric LOX flow $\dot{V}_{LOX}$ is measured by a turbine flow meter (Natec Sensors, type: NT-12, range: 1.1-80 l/min). For mass flow calculation, pressure and temperature sensors are installed upstream the turbine. GOX is liquefied in a double-walled run tank by liquid nitrogen (LN2) and pressurized by GOX. The main supply line downstram the supply valve and the injector are pre-cooled with LN2. Overpressure safety valves in the run tank and the main line prevent critical supply pressures. The injector can be purged with GN2.

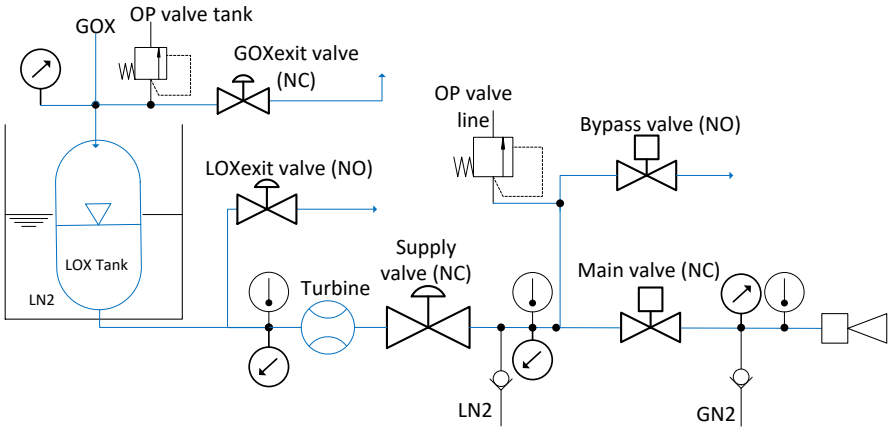

Fig. 5: Fluid schematic – LOX supply

3. Experimental results

In the following the test results will be presented beginning with the analysis of the LOX flow checks and followed by the hot tests, which are conducted with film and without film fluid.
Fig. 6 shows the experiment envelope with all operated points (‘x’) in blue and red. The envelope gives an overview over the absolute maximum static pressures and the mixture ratios. Tests without film coolant injection are limited to the selected operating points. For the 20 bar case with film an average absolute static pressure of 19.1 bar is achieved. Without film a decrease of 1.2% is obtained. For the 25 bar case with film a pressure of 23.5 bar is reached. Without film a drop of 1.6% is measured.

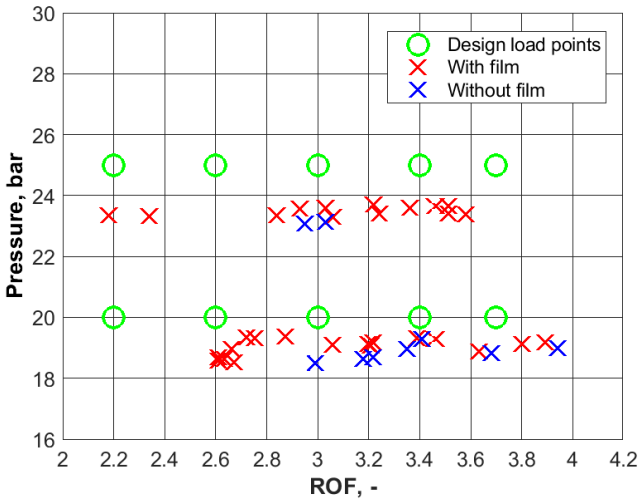

Fig. 6: Experiment envelope – Single element chamber – LOX/GCH4

In a shear coaxial injector, the mixing efficiency is mainly driven by the shear forces between the propellants. The velocity ratio VR between the methane and the LOX stream velocity [Eq. (1)] is used to characterize the injection conditions. For the film injection, a film velocity ratio VRF between the nitrogen and the methane stream velocity [Eq. (2)] is defined.

$$\mathrm{VR} = \frac{u_{GCH4}}{u_{LOX}} \quad \textbf{(1)}$$

$$\mathrm{VRF} = \frac{u_{GCH4}}{u_{film}} \quad \textbf{(2)}$$

DOI: 10.13009/EUCASS2019-144

As methane and nitrogen are in gaseous state, the VRF reveals a constant value of 1.78 with a deviation of ± 0.2. Including all tests at 20 bar and 25 bar the VR shows a linear behavior inversely proportional to the mixture ratio as displayed in Fig. 7. As the injection velocity of methane stays constant and the one for LOX increases, the VR for 25 bar shows an offset to 20 bar which is directly proportional to the relative pressure increase. The Reynolds number for LOX of each test is above $1 \cdot 10^5$, thus the flow is in the turbulent region.

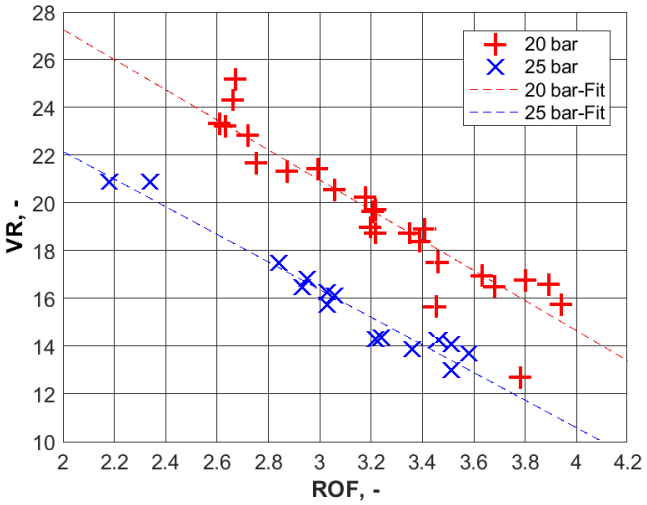

Fig. 7: Injector velocity ratio over the mixture ratio

To fully characterize the behavior of the shear coaxial injector, the individual discharge coefficents (C_d) and the pressure drop on the LOX side are calculated. Plotted over the normalized mass flows, Fig. 8 (left) presents on the one side the C_d values of the LOX injection tube in blue (flow checks) and red (hot tests), and on the other side the C_d values of the methane annulus (green) and methane orifice (magenta).
For the tested range the C_d value of LOX shows a constant behavior around 0.28 for the flow checks and 0.31 for the hot tests. The difference results from the increased back pressure via combustion. With 0.96 the methane orifice C_d value is close to the assumed value of 1.0 used for the load point calculations.
On the right of Fig. 8 the injector pressure drop of the LOX side is given for the flow checks (blue) and hot tests (red). The vertical lines (magenta) present the mixture ratio limits of the tested pressure levels (see Fig. 6). The pressure drop fitting curve (dashed blue) is a square root function, which is formed with the flow checks (blue ‘x’).

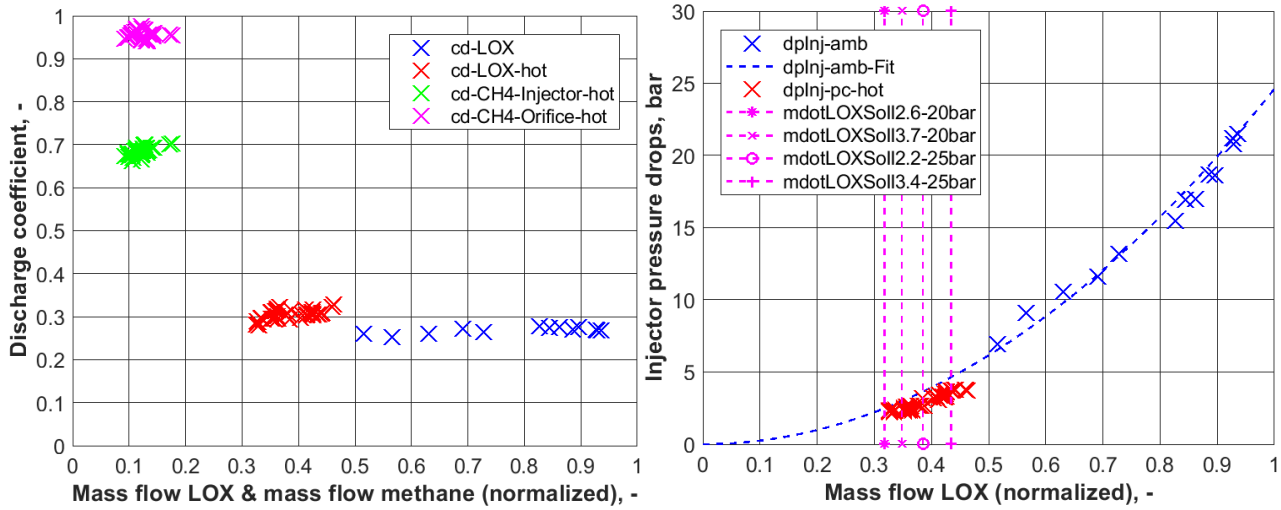

Fig. 8: Coefficients of discharge – Injector & methane orifice (left) – Pressure drops of the LOX injector (right)

On average the injector pressure drop normalized with the chamber pressure [Eq. (3)] is 13.0% at the 20 bar case and 14.9% at the 25 bar case.

$$\delta p_{inj} = \frac{\Delta p_{inj}}{p_c} \tag{3}$$

DOI: 10.13009/EUCASS2019-144

3.1 Experimental results – 20 bar

For analysis of the LOX supply, the cryogenic temperatures and pressures in the supply line and the LOX manifold are displayed over time in Fig. 9. The supply pressure at the turbine "PTurb" and the injector manifold "PLOXInj" is constant over the burn time ("PC101" = high). Due to the fluid flow the static pressure drop at the turbine is 0.1-0.2 bar, which is equal to the dynamic pressure. After the burn the manifold pressure increases due to a GN2 purge in order to get grid of the residual LOX in the fluid line. The same amplies to the methane supply.
For a detailed analysis of the temperatures Fig. 9 (right) just shows the cryogenic bulk temperature measurements at the tubine and the manifold. The flow check (between (1) and (2)), when "MVHVLOX" is high (dashed block) for the first time, sets the LOX bulk temperature in the manifold "TLOXInj" for the hot test (between (3) and (4)).
The temperature spikes at the LOX manifold ((2) and (4)) result from the instantaneous pressure drop in the manifold due to main valve closing after flow check and engine shut down. As the manifold pressure is at ambient condition before ignition, residual LOX in the manifold cools down to ambient conditions, as well (between (2) and (3)).
The temperature increase in the manifold at the flow check ((1)) and at ignition ((3)) results from fluid compression infront of the metal mesh, and from the inflow of heated LOX from the supply due to leakages in the isolation.
Leakage in the isolation is reasonalbe as the sensor upstream the turbine flow meter "TTurb" measures a temperature increase before (1) and (3).
The duration for the LOX temperature to reach steady state condition at combustion is ~1.5 s, thus a test evaluation at the last second of combustion is suitable. The temperature increase at the sensor "TTurb" during combustion is negligible.

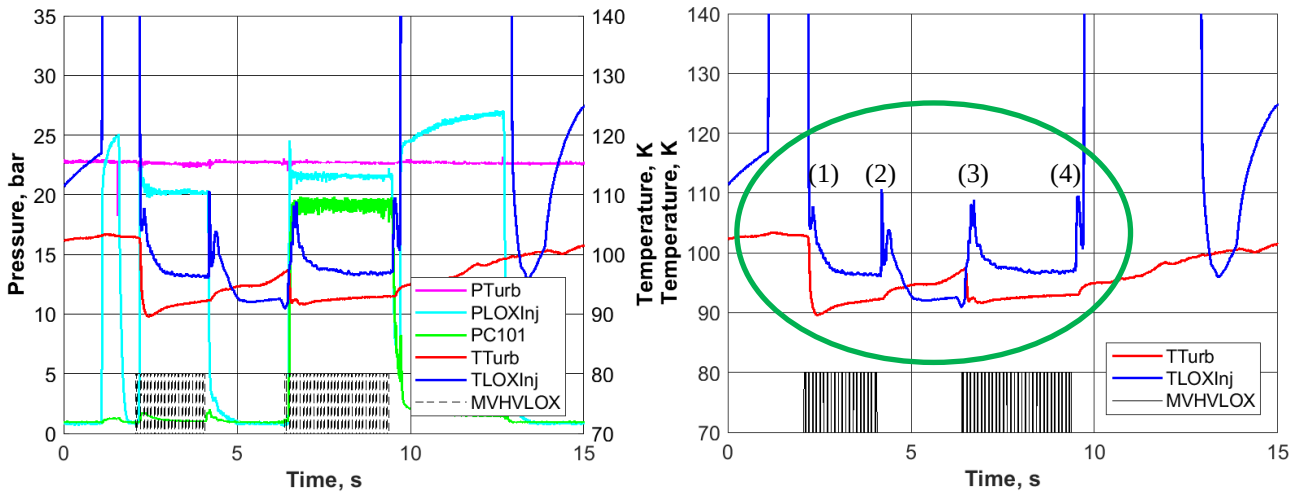

Fig. 9: Cryogenic bulk temperatures over time at the main valve and the injector manifold

For analysis of the chamber wall temperature distribution, a test executed with GN2 film at a mixture ratio of 3.0 is taken as a characteristic example. The chamber wall temperature over time at each position $T_i(t)$ is displayed as a relative value (see Fig. 10) and follows the equation:

$$\Delta T_{i,rel}(t) = T_i(t) - T_{i,ref} \qquad \text{with: } T_{i,ref} = T_i(t = 6.0\ s) \qquad \textbf{(4)}$$

$$t_{evaluation} = 8.5\ s$$

The red '∗' and '+' markers display the bottom wall temperature measurements in 1 mm distance to the hot gas wall over the chamber length. The cyan cirlce, magenta solid and the black diamond marker represent the top wall temperature sensors (see Fig. 10, left and Fig. 3). The maximum is reached at the last sensor of the first segment ("TCLU81"). In the second segment[2] the distribution is constant within a range of 14 K and a drop is seen as the result of the contact resistance of both segments at 145 mm. The constant trend indicates a fully developed heat release to the wall due to completed combustion in the second segment. The temperature fitting curve ("Fit-1 mm", dashed line) only refers to the rectangular combustion channel, the nozzle is not taken into account.
As the window block is an isolated body, the thermocouple measures a 15% higher value compared to the corresponding bottom wall sensor. In addition, the values at the top and the bottom wall at the same axial position are identical (see Fig. 10, left).

[2] The third last sensor seems to be not at its designated position or has a function problem as it is always measures up to 20 K lower temperatures than the rest of the sensors in the second segment.

DOI: 10.13009/EUCASS2019-144

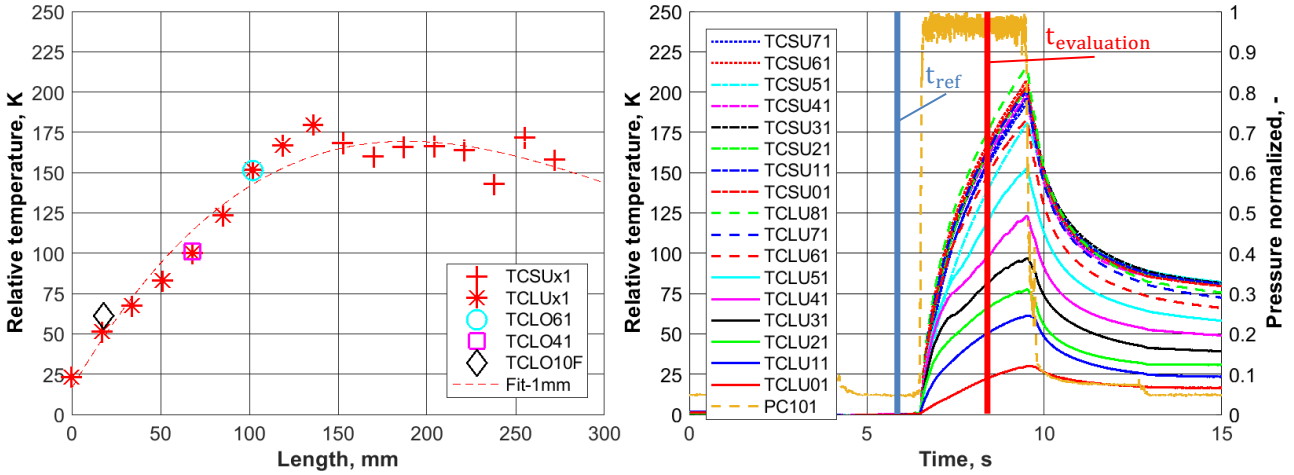

Fig. 10: Relative chamber wall temperatures over length (left, at $t_{evaluation}$) and over time (right)

The static chamber pressures are evaluated at $t_{evaluation}$ and averaged over ± 0.5 s. In Fig. 11 the chamber pressure distribution over length is plotted and normalized with the first pressure sensor "PC101". Compared to each other are three tests with different mixture ratios at the 20 bar level. The tests with film enabled are on the left, and without film are on the right. The maximum difference obtained at the last chamber position (270 mm) is less than 1% with film fluid. For the tests without film the chamber pressure distribution is identical for all viewed mixture ratios.

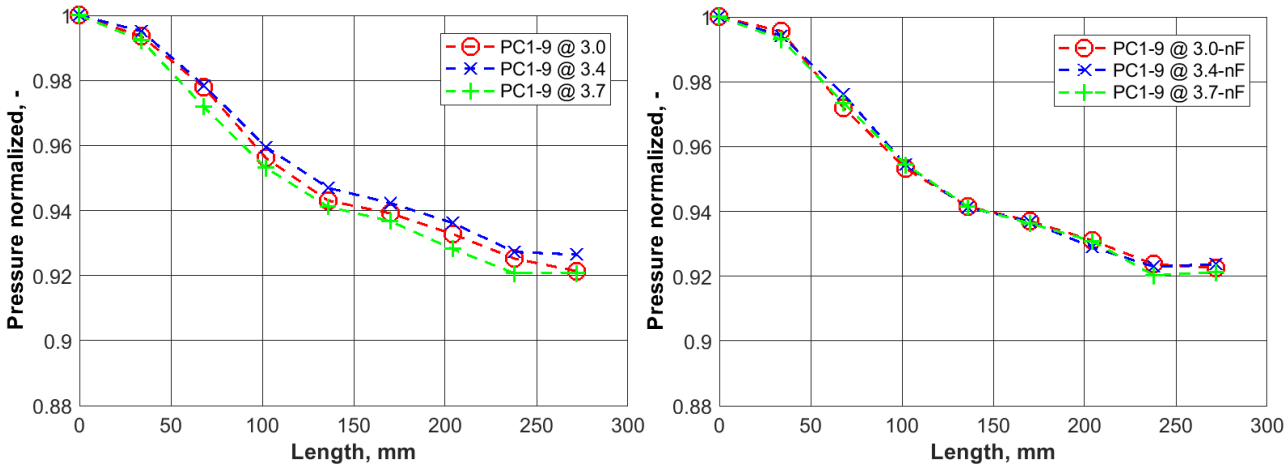

Fig. 11: Comparison of the normalized chamber pressure trend over length for different mixture ratios
20 bar – ROF=3.0-3.4-3.7 – With film (left) – Without film (right)

In general the pressure loss by combustion up to the last measured position is ~8%. ~75% of the total losses are obtained in the first segment. For the last two positions the loss is equal zero, thus a fully complete combustion is assumed.

On the opposite, an overall difference is not seen in the wall temperature distribution for different mixture ratios tested with film fluid at 20 bar. In comparison, without film a difference is seen for the wall temperatures in the second chamber segment. The deviation between the extremes of the mixture ratios is ~5%. The lowest maximum is reached at a mixture ratio of 3.0 (see Fig. 12).
In addition, without film an increase of the top wall temperature of 10% at the window and 11%, respectively 7% at the other two positions is measured, following the equation:

$$\theta_{i,rel,no\ film} = 100\% \cdot \frac{\Delta T_{i,rel,no\ film} - \Delta T_{i,rel,film}}{\Delta T_{i,rel,no\ film}} \quad \textbf{(5)}$$

DOI: 10.13009/EUCASS2019-144

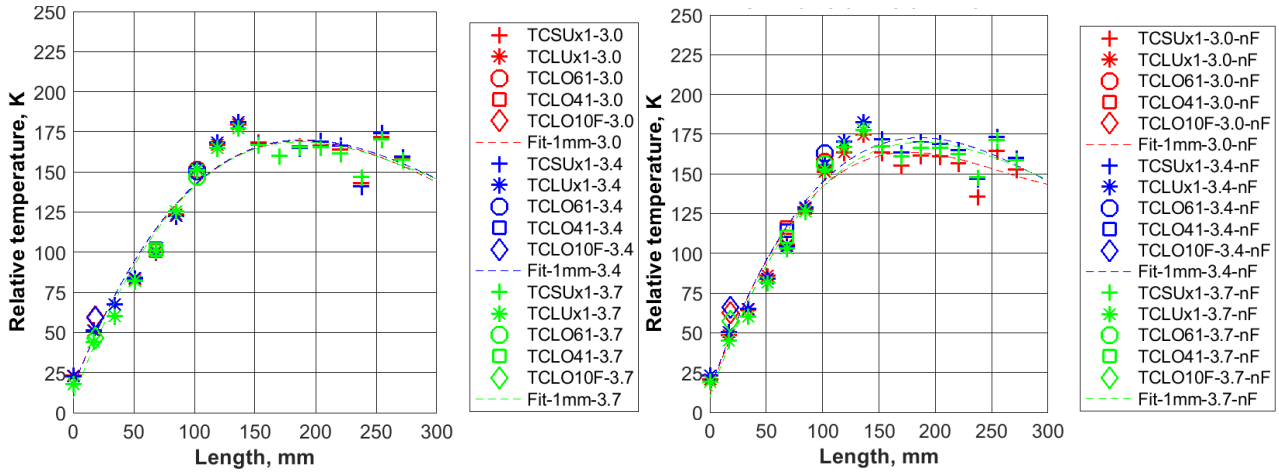

Fig. 12: Comparison of the relative chamber wall temperatures over length length for different mixture ratios
20 bar – ROF=3.0-3.4-3.7 – With film (left) – Without film (right)

3.2 Experimental results – Comparison 20 bar and 25 bar

In the following the 25 bar tests are compared to the 20 bar case. The pressure distribution and the chamber wall temperatures are investigated in detail for a mixture ratio of 3.0 with film and without film.
The static chamber pressure loss at 25 bar is in total equal to the 20 bar case as presented in Fig. 13. The last three sensors show a relative loss of less than 1% indicating a completed combustion or at least a fully developed heat release profile for the 25 bar case independent of the film fluid. From a local point of view (Fig. 13, right) the maximum difference between both pressure levels at the same position is 0.9% with film, respectively 0.5% without film fluid.

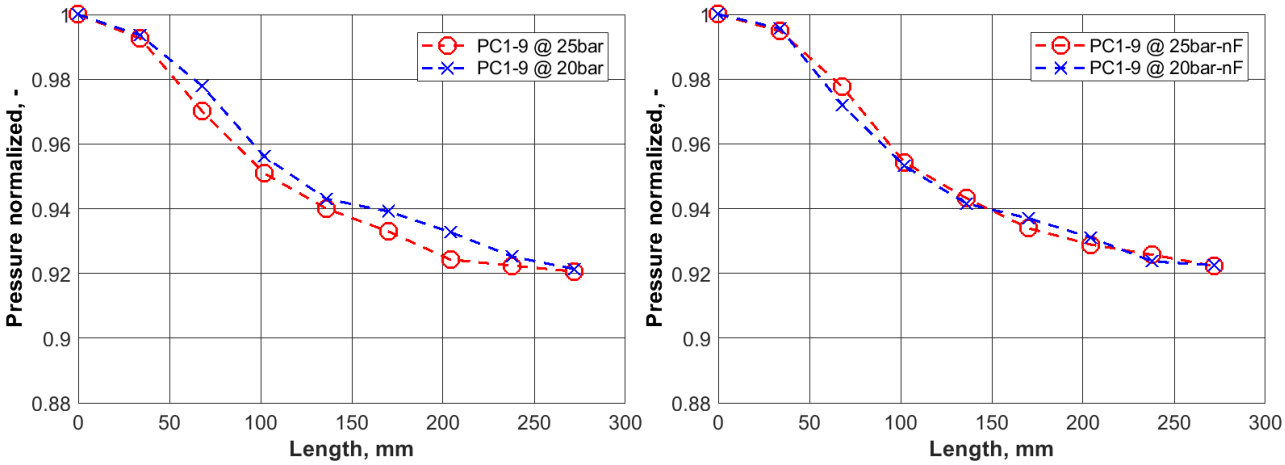

Fig. 13: Comparison of the normalized chamber pressure trend over length for 20 bar and 25 bar
With film (left) – Without film (right)

Fig. 14 presents the relative wall temperatures at the 20 bar pressure level on the left and at 25 bar on the right along the chamber length. Compared are tests with film to tests without film cooling.
Directly at the faceplate ($x = 0$), film or a different pressure level has no influence on the heat input.
At 20 bar and disabled film an increase of 5% is obtained at the window block, respectively 20% at 25 bar following [Eq. (5)]. This is a relative increase of 300% changing the pressure level. With the stainless steel window block the temperatures differences between tests with film enabled and disabled are assumed to be far higher as seen in [4].
In consequence film cooling is needed for low conduction coefficient materials like steel or glass to prevent overheating.
Downstream the window on the top wall an increase of 4-13% at 20 bar is calculated when film is disabled. In the case of 25 bar chamber pressure a rise of 6-8% is revealed without film. Thus, for the configuration tested the film effect seems to decay for higher chamber pressures but gets more efficient at the window block.
As seen in Fig. 10 the bottom and top wall temperatures at the same position are identical, when the film is enabled. A decline is actually expected for the top wall. Without film the top wall values are further increased (see Fig. 14, blue top wall markers). This is an indication for an unsymmetrical combustion flame, which points to the top wall.

DOI: 10.13009/EUCASS2019-144

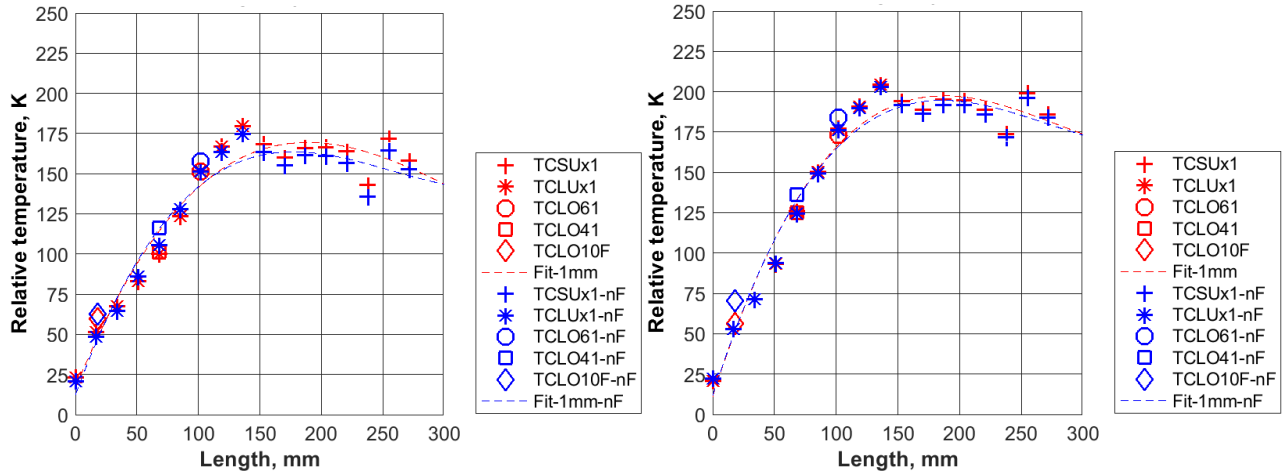

Fig. 14: Comparison of the relative chamber wall temperatures over length with film and without film
20 bar, ROF=3.0 (left) – 25 bar, ROF=3.0 (right)

In the second chamber segment the wall temperature maximum decreases ~3% without film at the 20 bar case and ~1% without film at the 25 bar case, thus the film has a minor influence on the overall chamber wall heat input.
By increasing the pressure, ~16% more heat input in the combustion chamber wall is measured at the extremes. This corresponds to the heat flux correlation[3] accurately [7]:

$$p_c^{0.8} \sim \dot{q} \sim \Delta T \quad \textbf{(6)}$$

with [8]:

$$\dot{q} = S \cdot \lambda \cdot \frac{\Delta T}{A_{hw}} \quad \textbf{(7)}$$

4. Outlook

On the left of Fig. 15 a characteristic high frequency pressure signal is plotted over time. The spike at the beginning is correlated to the ignition. The amplitude is random but ranges from 10 bar to 40 bar. On the right a nontypical pressure trend is displayed. For this test, at the evaluation range, the mixture ratio is 2.67 and the VR value is 25.20. Compared to nominal test the signal is 50% more rough in the second half of the combustion time.

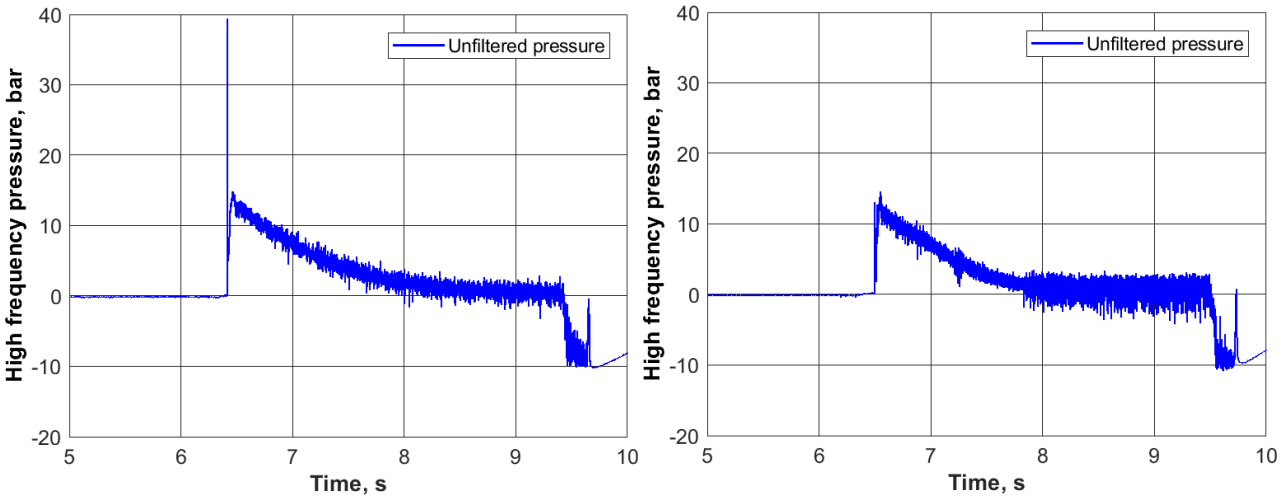

Fig. 15: High frequency pressure over time – Typical trend (left) – Nontypical trend (right)

[3] Calculation and analysis of the heat flux rate is ongoing.

DOI: 10.13009/EUCASS2019-144

Analysis of the frequencies, calculated via fast fourier transformation analysis[4] (see Fig. 16, left, window length: 0.1 s), shows a spike of 1800 Hz at 7.55 s which is assumed to be correlated to the first longitudinal mode (L1). The amplitude decays to the end of the test (see Fig. 16, right) as the mixture ratio is increasing (see Fig. 17).
In Fig. 17 the mixture ratio trend is plotted over the time of combustion ("MVHVLOX" = high). The increased amplitudes seem to appear at a mixture ratio of 2.5. More tests are needed to verify this behavior.

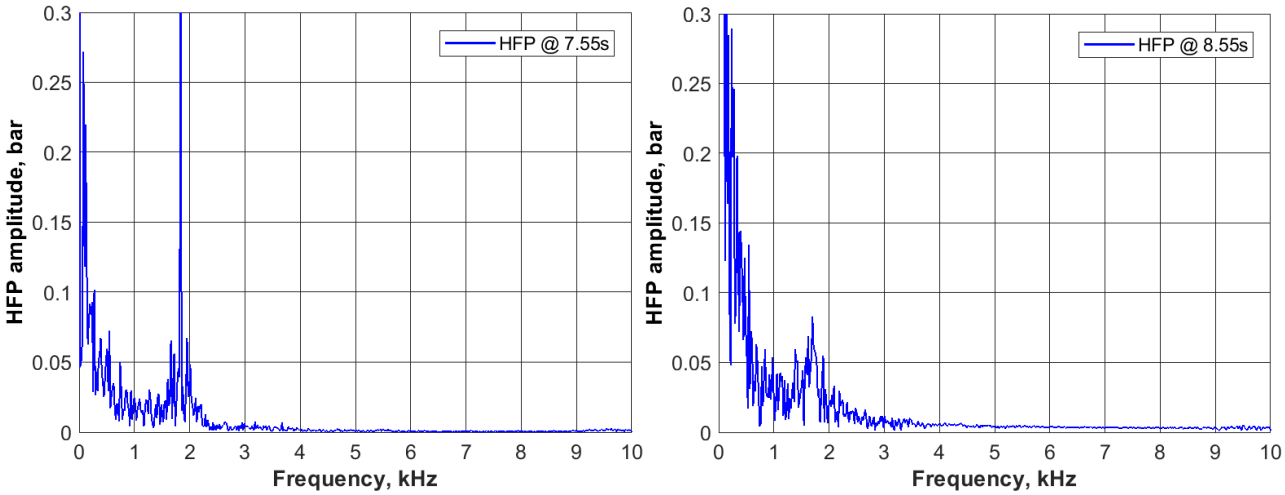

Fig. 16: FFT analysis – Window length = 0.1 s – Nontypical test

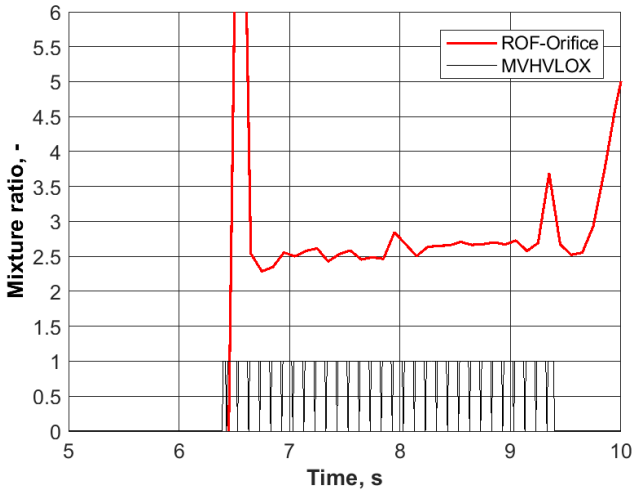

Fig. 17: Mixture ratio over time of the nontypical test

[4] Use of the "Kistler" HF pressure sensor. A more detailed analysis is ongoing.

DOI: 10.13009/EUCASS2019-144

On the data basis of the single injector element tests the future step is to prepare and test the water cooled subscale multi injector element combustion chamber "BKSC" (see Fig. 18). It features a new injector head for cryogenic application with seven shear coaxial injector elements with the identical geometry used for the single element chamber. The chamber segments and the faceplate are taken from the GOX/GCH4 assembly (see [3]).

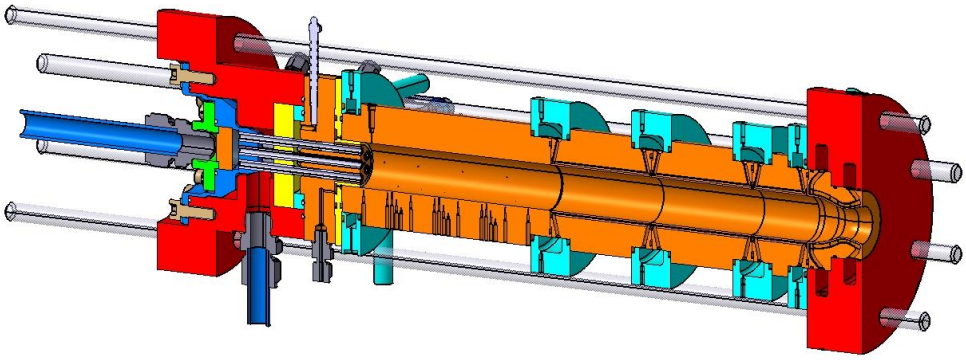

Fig. 18: Combustion chamber "BKSC" – Seven injector elements – LOX/GCH4

5. Conclusion

The test bench at the research center TUM in Garching is able to conduct tests using the propellant combination LOX/GCH4. For the driven envelope, the LOX injection temperature is far below the saturation temperature, thus 2-Phase flow in the LOX bulk can be excluded. Comparing the tests with film fluid to the tests without film show no major difference in the static pressure distribution. In addition, the wall temperatures for the tested mixture ratio range show a negligible deviation. Tests using a stainless steel window block should show a different behavior as the surface temperatures are expected to be higher, thus film cooling is necessary. Comparison of the two tested pressure levels revealed a similar distribution over time and length for the normalized pressure and for the wall temperatures with increased maximum temperatures of 16% for the 25 bar case. Before installing the round seven injector element combustion chamber, tests investigating the nontypical behavior and analysis of the heat flux rate are appropriate.

Acknowledgement

The activity is supported by the "Bavarian Research Foundation" and ArianeGroup GmbH.
The author would like to thank the PhD student Paul Lungu for the support provided during the test execution and analysis.

References

[1] M.P. Celano, S. Silvestri, G. Schlieben, C. Kirchberger and O.J. Haidn, 2013. Injector Characterization for a GOX-GCH4 Single Element Combustion Chamber. *5th European Conference For Aeronautics and Space Sciences (EUCASS), Munich, Germany*

[2] D. Preclik, O. Knab, G. Hagemann, C. Mäding, , D. Haeseler, O. Haidn, A. Woschnak, and M. De Rosa, 2005. LOX/Hydrocarbons Preparatory Thrust Chamber Technology Activities in Germany. *AIAA 2005-4555 41th AIAA/ASME/SAE/ASEE Joint Propulsion Conference and Exhibit, American Institute of Aeronautics and Astronautics, Tucson, AZ*

[3] S. Silvestri, M.P. Celano, G. Schlieben and O.J. Haidn, 2016. Characteriazation of a Multi-Injector GOX-GCH4 Combustion Chamber. *AIAA Paper 2016-4992*

[4] C.B. v. Sethe, 2016. Experimental feasibility study and implementation of an optically accessible single injector element GOX/GCH4 combustion chamber. Semester Thesis (TUM)

[5] F. Winter, N. Perakis, O.J. Haidn, 2018. Emission Imaging of a coaxial single-element GOX/GCH4 rocket combustor. *Joint Propulsion Conference*

[6] S. Silvestri, C. Kirchberger, G. Schlieben, M.P. Celano, O.J. Haidn, 2017. Experimental and Numerical Investigation of a Multi-Injector GOX-GCH4 Combustion Chamber. *31st ISTS*

[7] F.D.D. Incropera und T. Bergmann, 1981. Fundamentals of Heat and Mass Transfer.

[8] M.P. Celano, S. Silvestri, J. Pauw, N. Perakis, F. Schily, D. Suslov and O.J. Haidn, 2015. Heat Flux Evaluation Methods for a Single Element Heat-Sink Chamber. *6th European Conference For Aeronautics and Space Sciences (EUCASS)*